DOI: 10.1002/cbic.200800489

Extremely Tight Binding of a Ruthenium Complex to Glycogen Synthase Kinase 3

G. Ekin Atilla-Gokcumen,[a] Nicholas Pagano,[a] Craig Streu,[b] Jasna Maksimoska,[b] Panagis Filippakopoulos,[c] Stefan Knapp,[c] and Eric Meggers*[a]

The pharmaceutical industry and chemical biology are dominated by organic chemistry, with inorganic compounds playing only a minor role. This is well illustrated by a review of drugs approved by the FDA during 2007 in which not a single compound contains a metal atom, with most compounds being reversible enzyme inhibitors.[1] However, our laboratory recently demonstrated that chemically inert metal complexes can serve as promising scaffolds for the design of enzyme inhibitors, and we have reported several compounds with high affinities and promising selectivity profiles for protein kinases and lipid kinases.[2–4] For example, we have recently introduced the ruthenium half-sandwich complexes **HB12** and **DW12** (Scheme 1) as potent protein kinase inhibitors, in particular for GSK-3 and Pim-1.[5–7] **DW12** and its derivatives induce strong biological responses such as the activation of the wnt signaling pathway in mammalian cells, strong pharmacological effects during the development of frog embryos, and the efficient induction of apoptosis in some melanoma cell lines.[8,9]

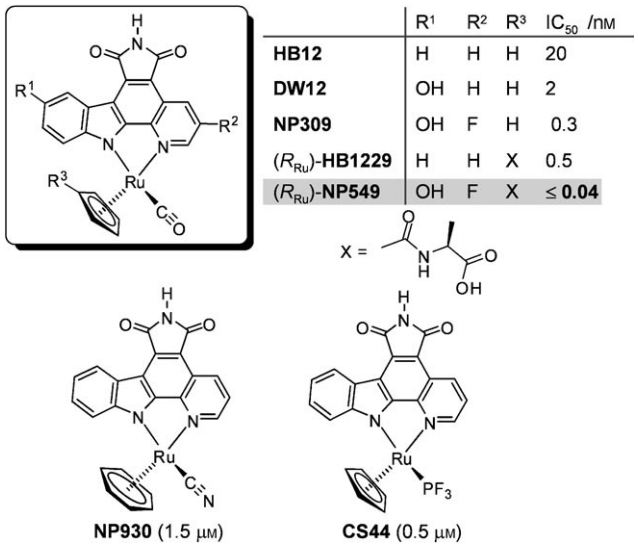

	R^1	R^2	R^3	IC_{50} /nM
HB12	H	H	H	20
DW12	OH	H	H	2
NP309	OH	F	H	0.3
(R_{Ru})-**HB1229**	H	H	X	0.5
(R_{Ru})-**NP549**	OH	F	X	≤ **0.04**

Scheme 1. Ruthenium complex **HB12** as a lead scaffold for the design of highly potent GSK-3 inhibitors. **NP930** and **CS44** are only weak inhibitors for GSK-3. IC_{50} values were measured at 100 μM ATP. Compounds are racemic if not indicated otherwise.

Here we present the extremely high-affinity organoruthenium inhibitor (R_{Ru})-**NP549** (Scheme 1), which displays at most low picomolar binding affinity for GSK-3, and report our elucidation of its binding to GSK-3β by X-ray crystallography. Compound (R_{Ru})-**NP549** is the result of a brief structure–activity relationship study starting with the plain scaffold **HB12**. We found that the introduction of a hydroxy group into the pyridocarbazole heterocycle, leading to **DW12** (IC_{50} = 2 nM), results in a tenfold increased potency for GSK-3.[6] Introduction of an additional fluorine at the pyridine moiety improved the binding affinity by almost another order of magnitude (**NP309**, IC_{50} = 0.3 nM).[10] Moreover, in an independent previous study we discovered by a combinatorial approach that the introduction of a D-alanine amide side chain onto the η^5-cyclopentadienyl moiety of **HB12** increased its affinity 40-fold ((R_{Ru})-**HB1229**).[11,12] In view of these results, we were curious to investigate by how much we could further improve potency if we were to combine these beneficial modifications at the cyclopentadienyl and pyridocarbazole moieties in one molecule. Accordingly, we synthesized the individual stereoisomers of **NP549** (see the Supporting Information for synthetic details) and found (R_{Ru})-**NP549** to be an extremely potent inhibitor for GSK-3β, with an IC_{50} of 40 pM at 100 μM ATP.[13,14] Since this IC_{50} was measured in the presence of the lowest practicably possible GSK-3β concentration of 100 pM, this value reflects an upper limit. Because GSK-3β displays a K_m value for ATP of 15 μM, the binding constant can be estimated as $K_i \leq 5$ pM by application of the Cheng–Prusoff equation.[15] With this value, (R_{Ru})-**NP549** is one of the highest-affinity ligands for a protein kinase known to date[16] (Figure 1).

In order to investigate the binding mode of this class of organoruthenium complexes to GSK-3β, we crystallized full-length human GSK-3β, soaked it with a solution of enantiomerically pure (R_{Ru})-**NP549**, and solved to a resolution of 2.4 Å (Table 1). The global structure reveals the typical two-lobe protein kinase architecture, connected by a hinge region, with the catalytic domain positioned in a deep intervening cleft and (R_{Ru})-**NP549** occupying the ATP-binding site, similar to the binding of staurosporine and synthetic organic inhibitors (Figure 2).[17]

Compound (R_{Ru})-**NP549** forms a number of hydrogen bonds within the ATP-binding site of GSK-3β (Figure 3). Together, the maleimide moiety and the indole OH group establish three important hydrogen bonds to the backbone of the hinge region:

[a] G. E. Atilla-Gokcumen, N. Pagano, Prof. Dr. E. Meggers
Fachbereich Chemie, Philipps-Universität Marburg
Hans-Meerwein-Strasse, 35043 Marburg (Germany)
Fax: (+49) 6421-282-1535
E-mail: meggers@chemie.uni-marburg.de

[b] C. Streu, J. Maksimoska
Department of Chemistry, University of Pennsylvania
231 S. 34th Street, Philadelphia, PA 19104 (USA)

[c] Dr. P. Filippakopoulos, Dr. S. Knapp
Centre for Structural Genomics, Oxford University
Botnar Research Centre, Oxford, OX3 7 LD (UK)

Supporting information for this article is available on the WWW under http://www.chembiochem.org or from the author.

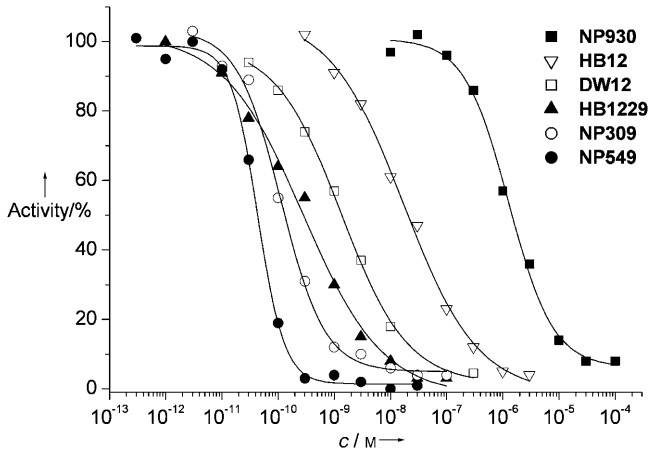

Figure 1. IC_{50} curves with GSK-3β obtained by phosphorylation of phosphoglycogen synthase peptide-2 with [γ-^{32}P]ATP at 100 μM ATP. **HB1229** and **NP549** were used as their R_{Ru} isomers.

Table 1. Crystallographic data and refinement statistics.

Parameter[a]	
space group	$P2_12_12_1$
cell dimensions [Å]	$a=83.04$, $b=86.11$, $c=177.39$
resolution [Å]	2.4
total observations (unique, redundancy)	209116 (52103, 4)
completeness (outer shell)	97.4 (98.3)
R_{merge} (outer shell) [%]	10.5 (71.2)
I/σ (outer shell)	14.4 (2.1)
R_{work} (R_{free}) [%]	19.0 (22.7)
hetero groups	(R_{Ru})-**NP549**
rmsd bond length	0.016
rmsd bond angle	1.548
Ramachandran (allowed/ generally allowed/disallowed)	91.1/8.6/0.3

[a] rmsd = root-mean-square deviation.

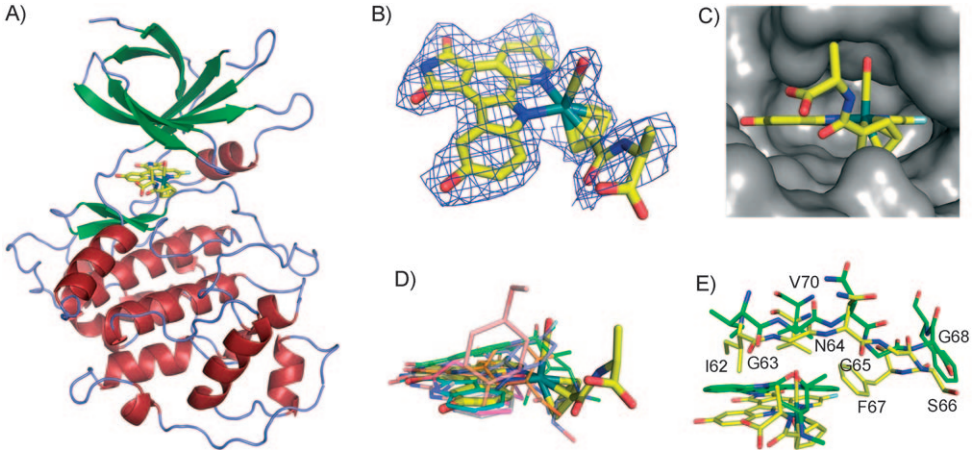

Figure 2. Crystal structure of GSK-3β with the ruthenium compound (R_{Ru})-**NP549** bound to the ATP-binding site. A) Overview of the complete structure. B) Electron density of the ruthenium complex contoured at 1 σ. C) Fit of (R_{Ru})-**NP549** into the active site of GSK-3β with emphasis on the hydrophobic pocket for the CO ligand. D) Superimposed binding positions of (R_{Ru})-**NP549** and other small molecules (PDB codes 1V5, 1Q3D, 1Q3W, 1Q4L, 1Q5K, 1Q41, and 1ROE) within the ATP-site of GSK-3β. E) Relative binding positions of (R_{Ru})-**NP549** and staurosporine (PDB code 1Q3D) within the ATP-site of GSK-3β.

one between the imide NH group and the backbone carbonyl oxygen of Asp133, a second between one of the imide carbonyl groups and the backbone NH of Val135, and the third between the backbone carbonyl oxygen of Val135 and the indole OH. The second carbonyl group of the maleimide moiety forms a water-mediated contact to Asp200. An additional hydrogen bond is established with the amide carbonyl group at the cyclopentadienyl moiety, which is in a water-mediated contact to Thr138. The carboxylate group does not form any particular hydrogen bond but is well placed close to a positively charged patch formed by Arg141 and Arg144, thus contributing to electrostatic attraction. Furthermore, the fluoride atom is close to the amino group of Lys85 (3.1 Å), which suggests a weak F···H–N hydrogen bond.

Compound (R_{Ru})-**NP549** is involved in extensive van der Waals contacts with GSK-3β. A hydrophobic pocket for the pyridocarbazole moiety is formed by side chains from more than 10 amino acids, in particular Phe67, Val70, Ala83, Val110, Leu132, Tyr134, Val135, Leu188, and Cys199. Phe67 also packs against the CO ligand and one edge of the cyclopentadienyl moiety, whereas Gln185 interacts with one edge and the face of the cyclopentadienyl ring and the adjacent amide carbonyl group. Finally, the methyl group of the cyclopentadienyl amide side chain forms a hydrophobic contact with the CH_2 group of Gly63 in the glycine-rich loop.

Most interestingly, the CO ligand comes into particularly close contact to Gly63, with a distance to the methylene group of only 3.1 Å. This is below the van der Waals distance and suggests dipolar interactions.[18] We have also observed such close contacts to glycine-rich loops in crystal structures of related organometallic compounds with the protein kinase Pim-1.[7,10] In addition, Gly63, together with the side chains of Ile62, Val70, and Phe67, create a small hydrophobic pocket in which the CO ligand is buried (Figure 3C). It is noteworthy that replacing the CO by any other monodentate ligand reduces the binding affinity significantly.[19] For example, exchanging the CO group in **HB12** for PF_3 (**CS44**) increases the IC_{50} around 25-fold, presumably because the PF_3 ligand is too big for this pocket, whereas replacing the (η^5-C_5H_5)RuCO moiety in **HB12** by the highly similar (η^6-C_6H_6)RuCN fragment (**NP930**) leads to a 75-fold diminished affinity (Scheme 1). Such a dramatic effect of the replacement of a CO ligand with a cyanide has also been observed by us previously in a related octahedral scaffold.[19] Although CO and cyanide are isoelectronic, coordinated CO is hydrophobic,[20,21] whereas coordinated cyanide tends to form hydrogen bonds with its nitrogen lone pair and

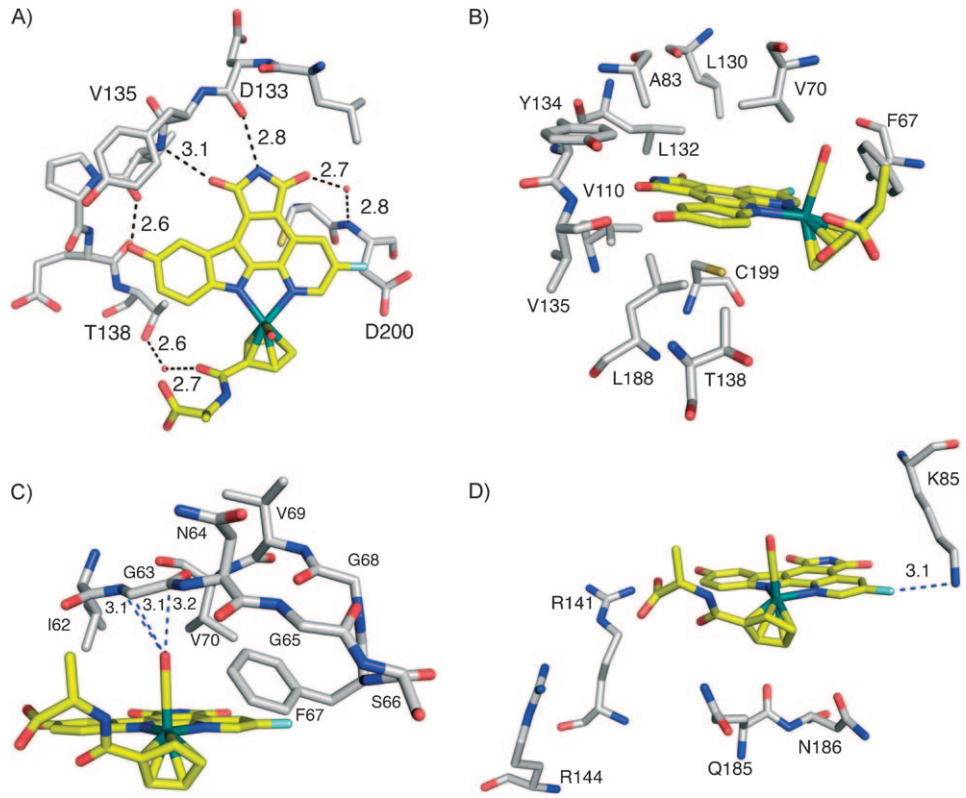

Figure 3. Interactions of (R_{Ru})-**NP549** within the ATP-binding site of GSK-3β. A) Hydrogen bonding interactions. B) The most important hydrophobic interactions. C) Highlighting the close contact of the CO ligand of (R_{Ru})-**NP549** with Gly63 and the small hydrophobic pocket for the CO. D) Proximity of the carboxylate to Arg141 and of Arg144 and of Lys85 to the fluorine substituent, together with interaction of Gln185 with the cyclopentadienyl ring and the adjacent amide carbonyl group.

should not therefore have any tendency to bind into the hydrophobic pocket formed from the glycine-rich loop.[22,23] These examples demonstrate the importance of the CO group, and we have in fact yet to find a highly potent and selective ruthenium complex for GSK-3 that lacks this apparently crucial CO ligand.

Finally, we compared the relative binding position of (R_{Ru})-**NP549** with cocrystal structures of small organic molecules bound to GSK-3β. A superimposition of all available structures demonstrates that (R_{Ru})-**NP549** occupies the same area of the ATP-binding site. However, it seems that the position of the CO ligand, together with the perpendicular orientation to the pyridocarbazole heterocycle, is a unique feature of (R_{Ru})-**NP549**, allowing Val70 to reach down to the pyridocarbazole moiety, thus maximizing the hydrophobic interactions with the pyridocarbazole moiety and creating the hydrophobic pocket for the CO ligand. Although the pyran oxygen atom of staurosporine occupies a position in the active site similar to that of the CO oxygen of the ruthenium complex, the glycine-rich loop is in a significantly more open position, as displayed in Figure 2E, and does not allow the same closure of the active site with its optimized contacts.

In conclusion, here we report an extremely high-affinity GSK-3 inhibitor and its binding to the ATP-binding site of GSK-3β. Overall, (R_{Ru})-**NP549** perfectly complements the shape of the ATP-binding site and forms three direct hydrogen bonds, two water-mediated hydrogen bonds, and one fluorine-mediated hydrogen bond, undergoes electrostatic contacts between the carboxylate tail and two arginines, and is involved in van der Waals interactions with over ten amino acids. Furthermore, the CO ligand stacks against the glycine-rich loop and is buried in a small pocket, which appears to be crucial for affinity and selectivity for GSK-3β. With a K_i value of around 5 pM or less, (R_{Ru})-**NP549** is one of the most potent protein kinase inhibitors reported to date, almost four orders of magnitude more potent than the related natural product staurosporine (IC_{50} = 180 nM at 100 μM ATP), demonstrating that this organoruthenium structure is a privileged scaffold for the design of GSK-3 inhibitors.

Experimental Section

Cloning, expression, purification, and crystallization of GSK-3β: GSK-3β was cloned into pET151 vector by use of a Champion™ pET Directional TOPO Expression kit (Invitrogen). The protein was expressed in Rosetta2DE3 cells as an N-terminal cleavable His_6-tag fusion protein with TEV cleavage site. The cells were grown at 37 °C until they reached O.D. = 0.4, at which point the temperature was decreased to 17 °C. Once the cells had reached OD = 0.6, protein expression was induced with isopropyl-β-D-thiogalactopyranoside (IPTG (1 mM) overnight. The next morning, the cells were centrifuged, resuspended in lysis buffer [HEPES (50 mM), pH 7.2, NaCl (50 mM), glycerol (5%)] and supplemented with Complete Protease Inhibitor Cocktail tablets (Roche). The cells were then lyzed by sonication at 4 °C. The supernatant was collected and subjected to ion-exchange chromatography (SP-Sepharose, GE Biosciences). The protein was bound onto the column in HEPES (50 mM, pH 7.2) and eluted with HEPES (50 mM, pH 7.2)/NaCl (1 M). The eluted fractions were applied to a Talon affinity column equilibrated with HEPES (50 mM, pH 7.5)/NaCl (300 mM). The column was washed with HEPES (50 mM, pH 7.5)/NaCl (300 mM)/imidazole (20 mM), and the protein was eluted with HEPES (50 mM, pH 7.5)/NaCl (300 mM)/imidazole (250 mM). GSK-3β was treated overnight with λ-phosphatase and TEV-protease to remove phosphate and His-tag, respectively. Further purification was achieved with a MONO-S column (GE Biosciences). The protein was loaded onto the MONO-S column in HEPES (50 mM, pH 7.2)/glycerol (10%)/dithiothreitol (DTT; 1 mM) and eluted with a linear gradient (0–1 M) of NaCl in HEPES (50 mM, pH 7.2), glycerol (10%), and DTT (1 mM) to ensure the separation of phosphorylated and non-phosphorylated species. Non-phosphorylated GSK-3β was sub-

jected to gel filtration chromatography (Superdex 26/60, GE Biosciences) in HEPES (50 mM), DTT (1 mM), $MgCl_2$ (2 mM), NaCl (500 mM), pH 7.2 and concentrated to 3–4 mg mL^{-1} for crystallization purposes. Crystals of the apo-protein were grown at 4 °C in 4 μL hanging drops in which protein solution (2 μL) was mixed with the precipitant solution (2 μL). Crystals were observed in Tris (100 mM, pH 7.2)/PEG 6000 (20%) or PEG 8000 (12.5%) within three days. The crystal quality was improved by overlaying oil (50% silicon oil in paraffin oil, 400 μL) onto reservoir solution (600 μL). Apo-form crystals were soaked with the ruthenium compound overnight at 4 °C in Tris (100 mM, pH 7.2), PEG 6000 (20%), (R_{Ru})-**NP549** (1 mM), DMSO (10%) and glycerol (1%). The next morning the crystals were cryoprotected in glycerol (25%) and flash frozen in liquid nitrogen.

Data collection and structure determination: Cryoprotected crystals diffracted up to 2.4 Å on the A1 beam line at the Cornell High Energy Synchrotron Source (Ithaca, NY). After indexing and merging of the data (HKL2000), the structure was solved by molecular replacement with use of a crystal structure of GSK-3β (PDB code ^{1}J1B) as a search model calculated with Phaser. Refinement and manual rebuilding of the model were performed with REFMAC5 and Coot, respectively. Data collection and current refinement statistics are listed in Table 1. Coordinates of the structure have been deposited in the Protein Data Bank (PDB ID: 2JLD).

Measurement of IC_{50} values with GSK-3β: GSK-3β and phosphoglycogen synthase peptide-2 (PGSP-2) were purchased from Upstate Biosciences (USA). Various concentrations of inhibitors were incubated at room temperature in 4-morpholinepropanesulfonic acid (MOPS; 20 mM), $MgCl_2$ (30 mM), BSA (0.8 μg $μL^{-1}$), and DMSO (5%, originating from the inhibitor stock solution) at pH 7.0, in the presence of PGSP-2 (20 μM) and GSK-3β (200 pM for **NP930**, **HB12**, and **DW12**; 100 pM for **HB1229**, **NP309**, and **NP549**). After 15 min, the reaction was initiated by addition of ATP (100 μM), including approximately 0.2 μCi $μL^{-1}$ [γ-^{32}P]ATP. Each reaction was performed in a total volume of 25 μL. After 60 min, the reaction was terminated by spotting of 17.5 μL of the reaction mixture onto a circular P81-phosphocellulose paper (diameter 2.1 cm, Whatman) followed by washing four times (five minutes each wash) with phosphoric acid (0.75%) and once with acetone. The dried P81-papers were transferred to a scintillation vial, and scintillation cocktail (4 mL) was added. The counts per minute (CPM) were determined with a Beckmann 6000 scintillation counter, and IC_{50} values were defined as the concentration of inhibitor at which the CPM was 50% of the control sample, corrected for the background.

Acknowledgements

We thank the US National Institutes of Health for support (GM071695).

Keywords: bioorganometallic chemistry · glycogen synthase kinase 3 · inhibitors · picomolar binding constant · ruthenium

[1] B. Hughes, *Nat. Rev. Drug Discovery* **2008**, *7*, 107–109.
[2] E. Meggers, *Curr. Opin. Chem. Biol.* **2007**, *11*, 287–292.
[3] E. Meggers, G. E. Atilla-Gokcumen, H. Bregman, J. Maksimoska, S. P. Mulcahy, N. Pagano, D. S. Williams, *Synlett* **2007**, 1177–1189.
[4] P. Xie, D. S. Williams, G. E. Atilla-Gokcumen, L. Milk, M. Xiao, K. S. M. Smalley, M. Herlyn, E. Meggers, R. Marmorstein, *ACS Chem. Biol.* **2008**, *3*, 305–316.
[5] H. Bregman, D. S. Williams, G. E. Atilla, P. J. Carroll, E. Meggers, *J. Am. Chem. Soc.* **2004**, *126*, 13594–13595.
[6] D. S. Williams, G. E. Atilla, H. Bregman, A. Arzoumanian, P. S. Klein, E. Meggers, *Angew. Chem.* **2005**, *117*, 2020–2023; *Angew. Chem. Int. Ed.* **2005**, *44*, 1984–1987.
[7] J. É. Debreczeni, A. N. Bullock, G. E. Atilla, D. S. Williams, H. Bregman, S. Knapp, E. Meggers, *Angew. Chem.* **2006**, *118*, 1610–1615; *Angew. Chem. Int. Ed.* **2006**, *45*, 1580–1585.
[8] G. E. Atilla-Gokcumen, D. S. Williams, H. Bregman, N. Pagano, E. Meggers, *ChemBioChem* **2006**, *7*, 1443–1450.
[9] K. S. M. Smalley, R. Contractor, N. K. Haass, A. N. Kulp, G. E. Atilla-Gokcumen, D. S. Williams, H. Bregman, K. T. Flaherty, M. S. Soengas, E. Meggers, M. Herlyn, *Cancer Res.* **2007**, *67*, 209–217.
[10] N. Pagano, J. Maksimoska, H. Bregman, D. S. Williams, R. D. Webster, F. Xue, E. Meggers, *Org. Biomol. Chem.* **2007**, *5*, 1218–1227.
[11] H. Bregman, E. Meggers, *Org. Lett.* **2006**, *8*, 5465–5468.
[12] The absolute configuration at the ruthenium has been assigned according to the priority order of the ligands being η^5-C_5H_5 > pyridine [N(C, C, C)] > indole [N(C, C, lone pair)] > CO.
[13] The diastereomer (S_{Ru})-**NP549** is a weaker inhibitor for GSK-3β, with an IC_{50} value of 220 pM at 100 μM ATP.
[14] The absolute configuration at the ruthenium center was assigned from the crystal structure of (R_{Ru})-**NP549** with GSK-3β.
[15] Y.-C. Cheng, W. H. Prusoff, *Biochem. Pharmacol.* **1973**, *22*, 3099–3108.
[16] For reversible low-picomolar protein kinase inhibitors, see: a) D. W. Fry, A. J. Kraker, A. McMichael, L. A. Ambroso, J. M. Nelson, W. R. Leopold, R. W. Connors, A. J. Bridges, *Science* **1994**, *265*, 1093–1095; b) A. J. Bridges, H. Zhou, D. R. Cody, G. W. Rewcastle, A. McMichael, H. D. Showalter, D. W. Fry, A. J. Kraker, W. A. Denny, *J. Med. Chem.* **1996**, *39*, 267–276; c) A. J. Bridges, *Chem. Rev.* **2001**, *101*, 2541–2571.
[17] For cocrystal structures of organic compounds with GSK-3β, see: a) J. A. Bertrand, S. Thieffine, A. Vulpetti, C. Cristiani, B. Valsasina, S. Knapp, H. M. Kalisz, M. Flocco, *J. Mol. Biol.* **2003**, *333*, 393–407; b) L. Meijer, A. L. Skaltsounis, P. Magiatis, P. Polychronopoulos, M. Knockaert, M. Leost, X. P. Ryan, C. A. Vonica, A. Brivanlou, R. Dajani, C. Crovace, C. Tarricone, A. Musacchio, S. M. Roe, L. Pearl, P. Greengard, *Chem. Biol.* **2003**, *10*, 1255–1266; c) R. Bhat, Y. Xue, S. Berg, S. Hellberg, M. Ormo, Y. Nilsson, A. C. Radesater, E. Jerning, P. O. Markgren, T. Borgegard, M. Nylof, A. Gimenez-Cassina, F. Hernandez, J. J. Lucas, J. Diaz-Nido, J. Avila, *J. Biol. Chem.* **2003**, *278*, 45937–45945; d) H. C. Zhang, L. V. Bonaga, H. Ye, C. K. Derian, B. P. Damiano, B. E. Maryanoff, *Bioorg. Med. Chem. Lett.* **2007**, *17*, 2863–2868.
[18] For orthogonal multipolar interactions in crystal structures, see: R. Paulini, K. Müller, F. Diederich, *Angew. Chem.* **2005**, *117*, 1820–1839; *Angew. Chem. Int. Ed.* **2005**, *44*, 1788–1805.
[19] See also: H. Bregman, P. J. Carroll, E. Meggers, *J. Am. Chem. Soc.* **2006**, *128*, 877–884.
[20] I. Ott, B. Kircher, R. Dembinski, R. Gust, *Expert Opin. Ther. Pat.* **2008**, *18*, 327–337.
[21] For hydrophobic interactions of CO bound to a heme-containing transcriptional activator, see: H. Youn, R. L. Kerby, G. P. Roberts, *J. Biol. Chem.* **2003**, *278*, 2333–2340.
[22] This is comparable to the nonproteic cyanide and CO ligands bound to iron in the active sites of hydrogenases. Whereas the cyanides are involved in specific hydrogen bonding interactions, the CO ligands are surrounded by hydrophobic residues. See, for example: M. Frey, *ChemBioChem* **2002**, *3*, 153–160.
[23] For the protonation of coordinated cyanides in the presence of a CO ligand, see, for example: C.-H. Lai, W.-Z. Lee, M. L. Miller, J. H. Reibenspies, D. J. Darensbourg, M. Y. Darensbourg, *J. Am. Chem. Soc.* **1998**, *120*, 10103–10114.

Received: July 17, 2008
Published online on November 26, 2008

